Periodicity doubling cascades: direct observation in ferroelastic materials

Arnoud S. Everhardt,[1,*] Silvia Damerio*,[1,†] Jacob A. Zorn,[2] Silang Zhou,[1] Neus Domingo,[3] Gustau Catalan,[3,4] Ekhard K. H. Salje,[5] Long-Quing Chen,[2] and Beatriz Noheda[1,6,‡]

[1] *Zernike Institute for Advanced Materials, University of Groningen, The Netherlands*
[2] *Department of Materials Science and Engineering, The Pennsylvania State University, University Park, Pennsylvania 16802, USA*
[3] *Catalan Institute of Nanoscience and Nanotechnology (ICN2), Spain*
[4] *ICREA, 08193 Barcelona, Spain*
[5] *University of Cambridge, UK*
[6] *CogniGron Center, University of Groningen, The Netherlands*

(Dated: May 6, 2019)

Very sensitive responses to external forces are found near phase transitions. However, transition dynamics and pre-equilibrium phenomena are difficult to detect and control. We have observed that the equilibrium domain structure following a phase transition in ferroelectric/ferroelastic $BaTiO_3$, is attained by halving of the domain periodicity multiple times. The process is reversible, with periodicity doubling as temperature is increased. This observation is reminiscent of the period-doubling cascades generally observed during bifurcation phenomena and, thus, it conforms to the 'spatial chaos' regime earlier proposed by Jensen and Bak[1] for systems with competing spatial modulations.

Keywords: ferroelastic thin films; domain dynamics; domain patterns; periodicity doubling; bifurcation

Current interest in adaptable electronics calls for new paradigms of material systems with multiple metastable states. Functional materials with modulated phases bring interesting possibilities in this direction[1]. Ferroic materials are good prospective candidates because the modulation can be controlled by external magnetic, electric or stress fields. In magnetic materials, the presence of competing interactions can lead to wealth of modulated structures, exemplified by the axial next-nearest-neighbor Ising (ANNNI) model [2]. In ferroelectrics, interesting modulations in the form of domain patterns involve not only domains with alternating up and down polarization but also vortices [3] and ferroelectric skyrmions [4]. Ferroelectrics are often also ferroelastic [5] and display modulations of the strain.

When ferroelastic materials are grown in thin film form on a suitable crystalline substrate, they can be subjected to epitaxial strain, which typically relaxes by the formation of ferroelastic domains [6, 7]. In the simple case of ferroelastic systems with orthogonal lattices grown on a cubic substrate, different types of 90° domain configurations form, either so-called *a/c* domains (with the long c-axis alternating in-plane and out-of-plane) or *a/b* domains (long axis fully in-plane), depending on the sign of the strain imposed on the film by the substrate [8]. In the absence of dislocations or other defects, ferroelastic domains in epitaxial films are expected to alternate periodically [6–8].

The periodicity of this modulation, or the domain width (w), is determined by the competition between the elastic energy in the domains and the formation energy of domain walls and is a function of the thin film thickness (d). For $d > w$, the relation $w = \beta d^{1/2}$ holds, as a particular case of the Kittel's law [6, 9–11]. In the ferroelastic case, geometrical effects are also important and discretization of domain widths, with minimum sizes determined by the need of lateral lattice coherence at the domain wall, have also been shown [12, 13]. Recently, an original hydrodynamics-like approach has been put forward, in which non-equilibrium ferroic domain structures are rationalized with respect to surface folding, wrinkling and relaxation [14].

As both misfit strain and domain wall energies change with temperature, the equilibrium patterns are temperature dependent and the question arises of how does the system evolves towards (global or local) equilibrium. While studies of ferroelectric domain formation and switching are common [15–20], less attention has been paid to microscopy studies of temperature-driven annihilation of ferroelastic nanodomains [21, 22] and it is only recently that experimental developments have allowed the *in-situ* study of domain dynamics [23–28].

In the present work, we report the direct observation of ferroelastic/ferroelectric domain evolution by sequential periodicity halving and doubling on $BaTiO_3$ thin films. Moreover, we present the results of phase field simulations [29–32] that support the observations showing that domain wall nucleation takes place in the center of existing domains. Period doubling cascades, associated to the proximity of order-to-chaos transitions, have been often observed as frequency doubling sequences in the time regime, but they have not yet been reported in spatially modulated systems. The results, thus, present strong evidence that ferroelastic systems with competing modulations are at the edge of chaos, as predicted for

* Equal contribution; Presently at: Materials Science Division, Lawrence Berkeley National Laboratory, Berkeley, CA 94720, USA
† s.damerio@rug.nl
‡ b.noheda@rug.nl

magnetic materials by Jensen and Bak [1].

The experiments have been performed on $BaTiO_3$ films grown under low epitaxial strain on $SrRuO_3$-buffered $NdScO_3$ substrates, as described in Ref.[33]. The low-strain condition flattens the energy landscape such that different ferroelectric domain configurations can be accessed within a moderate temperature range [34]. In particular, the films display a paraelectric-ferroelectric phase transition at 130 °C and a second transition at about 50 °C. The latter takes place in between two quite complex ferroelectric and ferroelastic phases (see Supplementary Material-section I for details) but, for the sake of clarity, it can simply be described as a transition from a high-temperature, pseudo-tetragonal a/c domain structure to a low-temperature, pseudo-orthorhombic a/b domain structure [35]. Unlike in other ferroics, the transformation from a/c to a/b domains in these films is slow enough to be followed with piezoresponse force microscopy (PFM) (see Supplementary Material-section II.a for details).

Typical domain configurations below and above the transition can be seen in the insets of Fig.1 a and b, at 25 °C and 70 °C, respectively. Inset in Fig.1 a shows a/b domains with domain walls projections parallel to the [110] direction. Inset in Fig.1 b shows a/c domain walls with projections parallel to the [010] direction. Investigation of a large number of samples with thicknesses ranging from 30 nm to 330 nm confirms the robustness of the domain configurations and the expected $w = \beta d^{1/2}$ scaling law, with $\beta \sim 10$ nm$^{1/2}$ for both the a/b and a/c domains, as shown in Fig.1. Here, the a/c structure refers to the domains generated while cooling from the paraelectric phase. When the a/c domain configuration is reached upon heating from the low-temperature a/b configuration, β is reduced to ~ 7 nm$^{1/2}$, reflecting the important role of pre-existing domain walls in the nucleation of new domain walls (see Supplementary Material-section III for details).

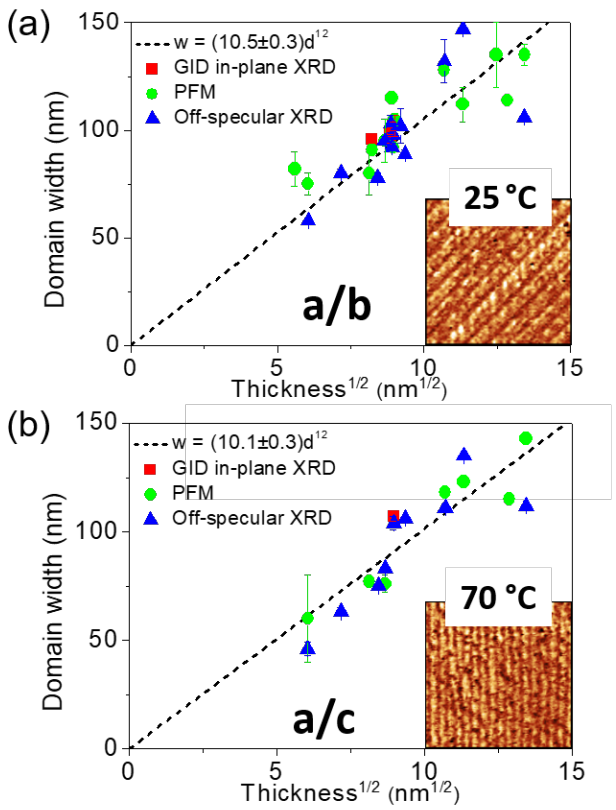

FIG. 1. Domain widths for different film thicknesses, determined by Grazing Incidence Diffraction (GID) XRD, off-specular XRD around the (204) Bragg peaks or PFM (see ref.[33]). The data are fitted to a square-root law with parameter β shown in the legend for the a/b (a) and the a/c (b) domain states. The insets show amplitude LPFM images of a 80 nm thick $BaTiO_3$ film at 25°C (a) and 70°C (b). The images are of a 1μmx1μm area with the edges along [100] and [010].

In order to investigate the evolution of the domain formation, the films were heated to 200 °C and measured during cooling. During the cool-down process, the a/c structure arises below the para-ferro transition. At a temperature of 70 °C, the first b-domains start appearing inside the a/c matrix and, increasing in number as the temperature lowers. Fig.2 shows images of two stages of the domain evolution taken while cooling with 5 °C steps. At 50 °C (Fig.2a), a/b and a/c domain walls coexist. The a/b domain walls, signalled with dashed lines, reveal a domain periodicity of (500 ± 50) nm for this 170 nm thick film. The periodicity values are obtained by performing the Fast Fourier Transform (FFT) of the LPFM images (see Supplementary Material-section II.a for details). Further cooling down to 30 °C (Fig.2b) shows new b-domains appearing halfway in between the existing domain walls, halving the domain periodicity to (250 ± 20) nm. This value is, in turn, approximately double that found at room temperature, after the sample has equilibrated for several hours and the high-temperature domain configuration has disappeared (see inset of Fig.1a). Thus, two sequential periodicity halving events take place during the transition from the a/c to the a/b domain configuration on cooling.

A similar mechanism, albeit shifted in temperature due to thermal hysteresis, is observed when heating the samples through the phase transition, as shown in Fig.3. The transition from a/b to a/c domains is followed on heating from 30 °C to 70 °C at 5 °C steps. The initial a/b domain periodicity at 30 °C is $w_0 = 100$ nm for a sample with thickness of 90 nm (Fig.3a). The domain walls start to rearrange and at 60 °C (Fig.3b), domains with $w = 2w_0$ are visible, as indicated by the green arrows. With increasing temperature up to 65 °C (Fig.3c), $w = 4w_0$ becomes the most abundant period (blue arrows) (see FFT in Fig.3d). In addition, a domain with a size of $w = 8w_0$ (violet arrow) can be observed within the area of the image (See Supplementary Material, section III, for the FFT of all three images). So the transition

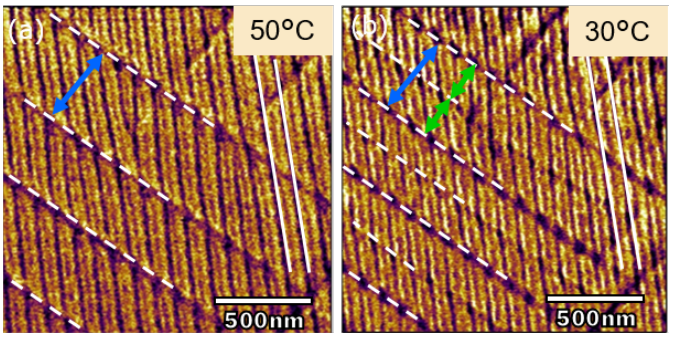

FIG. 2. Amplitude lateral PFM (LPFM) images of a 170 nm thick $BaTiO_3$ film on a $NdScO_3$ substrate. The transition from a/c to a/b domains is followed on cooling and images are shown in the coexistance regime at 50 °C (a) and 30 °C (b). The dashed lines indicate the a/b domain walls, whose in-plane projections are parallel to the $[\bar{1}10]$ direction; while the solid lines indicate two a/c domain walls, with in-plane projection parallel to the [010] direction. The blue double arrows signal the initial periodicity of $w_0 \sim 500$ nm. At 30°C, new a/b domains appear in the center of the existing domains. The green double arrows in (b) indicate the observed a/b domains with $w = 0.5w_0 \sim 250nm$

.

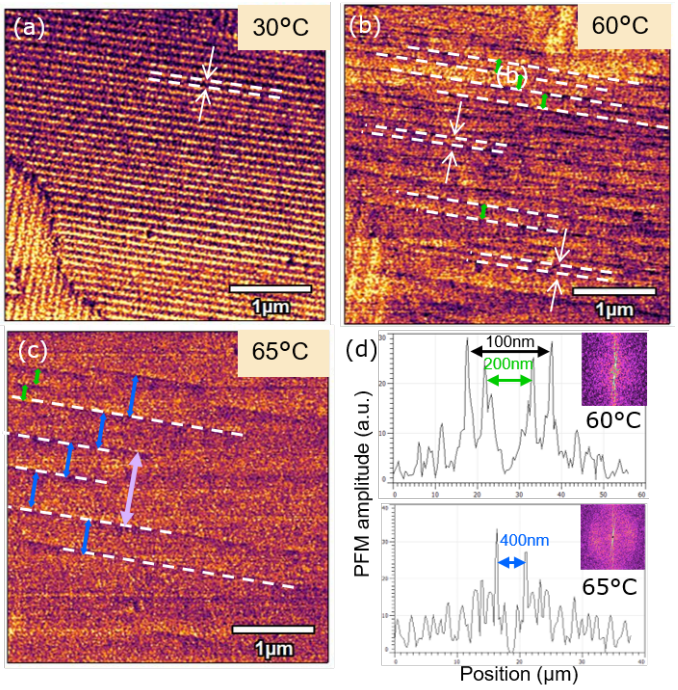

FIG. 3. Amplitude of the LPFM signal of a 90 nm thick $BaTiO_3$ film on a $NdScO_3$ substrate measured during heating at 30 °C (a), 60 °C (b) and 65 °C (c). (d) FFT of the images in (b) and (c), from which the domain period is determined. The basic domain width $w_0 = 110$ nm is indicated by the white arrows in (a) and (b). Other detected periodicities are $w = 2w_0 = 200$ nm (green) in (b) and (c), as well as $w = 4w_0 = 400$ nm (blue). A domain with size $w = 8w_0 = 800$ nm (violet) is also observed in (c).

to the a/c phase takes place by sequentially annihilating one every other b-domain and, thus, the apparent domain periodicities follow a Cantor set sequence with $w = 2^n w_0$ [36]. Pre-fractal domain patterns following Cantor set sequences have been observed in ferroelectrics under electric field [37]. Subsequent periodicity doubling events in these material have also been observed by reciprocal space mapping (see Supplementary Materials, section IV, for further details).

Our experiments also show the self-repairing of 'wrongly' nucleated domain walls, indicating that the center of existing domains is the equilibrium position for new domains. Fig.4a shows b-domains right after their formation, displaying unequal widths, probably due to pinning by the local defect structure. However, the elastic forces in this situation lead to a movement of the b-domains with respect to each other to reach a position equidistant between the neighboring b-domains (Fig.4b). It is well known that defects act as preferred nucleation points for new domains [11, 38], as observed in Fig.2a, where a defect (two a/c domains merging into one) close to the center of an a-domain induces the bending of the new wall in Fig.2b. Due to the random nature of these defects, we have occasionally observed deviations from the apparent 2^n domain evolution law.

Phase-field simulations are performed using the time-depedent Ginzburg-Landau equations for $BaTiO_3$ under strain (see Supplementary Material-Section II.b for details) and the results are shown in Fig.5. It is seen that the alternating pseudo-a/b phase appears at low temperatures and an a/c tetragonal structure predominates at

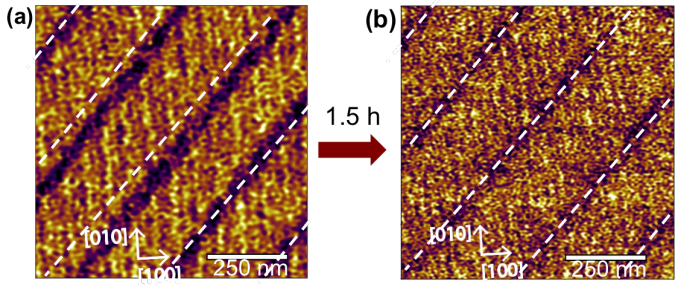

FIG. 4. LPFM amplitude images of a 170 nm thick $BaTiO_3$ film. (a) shows five different b-domains (darker diagonal bands) with different separations (a-domain widths). (b) After waiting for 1.5 hours, the domain walls re-arrange towards achieving a periodic configuration. The dashed lines signal the position of the b-domains in the ideal periodic case.

high temperatures. Fig.5a shows that the domain structure of the high temperature phase, a/c, agrees with the experimental observations previously captured by Everhardt *et al.* [33] with {101} domain walls (thus consistent with the [010] projections on the PFM images). These simulations also demonstrate the change in domain wall orientation from {101} to {110}, also consis-

tent with PFM observations, with the 'new' (orthorhombic) domains forming in the middle of the 'old' (tetragonal) domains. An analysis of the phase-field simulation results in a β coefficient of β=7nm$^{1/2}$ at high temperature and β =10nm$^{1/2}$ at low temperature, supporting our experimental observations in Fig.1).

Investigation of the elastic energies agrees with the experimental observation of stress relaxation being achieved by the formation of new domains at the center of old domains. To increase the simulation areas, we have also performed 2D simulations (see Fig.5b). In this case, the orientation of the polarization in the two phases does not fully agree with the experiment due to the simplicity of the model, but successive nucleation of new domains halfway between existing domain walls is clearly observed as the temperature is decreased. In addition, it is shown that the 'new' domains nucleate near the film-substrate interface, at the 90° (100) domain wall and along the $< 110 >$ directions.

Thus, periodicity changes take place by the formation of new stress-relieving elements (singularities) exactly in the center of the old domains, as already predicted by dynamic pattern formation [39, 40]. In the current measurements, a new b-domain (thus, a pair of domain walls) conforms such singularity, but other types such as single domain walls, dislocations, cracks, etc. are governed by similar physics. In the case of ferroelastic domains, increasing the strain (e.g. by decreasing the temperature) would repeat the process between a first-generation singularity and a second generation singularity, and so on.

More generally, in addition to boundary conditions and the effect of substrates, effective interactions between domain walls and evolution of domain wall structures can come from other physical processes. If several order parameters are activated to generate a domain wall, the energy landscape is complex with several minima, which combine to define the domains and the wall structures. Lateral extensions of domain walls would favour the wall-wall interactions and such phenomena have been explored in bi-quadratic or linear quadratic coupling between order parameters [41–46]. Atomistic approaches are very limited [47, 48] so far and no firm conclusions can be reached for direct interactions. If no such wall-wall interaction existed and no external constraints occur, then the pattern energy density would depend only on the total number of domain walls and their self-energy.

Periodicity can also originate from nucleation. Domains nucleate from the surface or an interface and the nucleation centres repel each other. The periodicity and deviations from a periodic array stem from the mistakes in distribution of nucleation sites, which would often form Cantor sets leading to phenomena like period doubling and local periodicity disorder [49–51]. Finally, we mention that in free crystals periodicity of domain walls, period doubling and disorder can be induced by the sideways movement of domains in terms of front propagation [40, 45, 52, 53].

Recent work [54–56] shows that, during the ferroelectic phase transition at 120 °C, $BaTiO_3$ crystals display transient intersections between polar ferroelastic/ferroelectric 90° walls and the (001) surface that are electrically charged and persist up to temperatures above T_C, while the bulk has already transformed into the cubic phase. Interestingly, a sequential period halving evolution in which some domains are missing during the cooling down process, most likely due to the local presence of other type of defects taking care of the stress relaxation, can explain the *discretization* of domain sizes that we have detected in various ferroelastic materials [57–61](see Supplementary Material- section V).

In conclusion, we directly observe spatial period doubling/halving sequences consistent with those found as part of the clock-model calculations [62]. This behavior belongs to a class of scaling phenomena known as period-doubling cascades that are mathematically investigated by means of bifurcation theory and characterize systems at the 'edge-of-chaos'. Even though a link with spatially modulated phases of matter has been made [1], spatial period doubling cascades had not yet been observed experimentally. Thus, our observation of domain periodicity halving should not be exclusive of the system under investigation, but represents a more general mechanism of transformation in materials with competing periodic structures.

ACKNOWLEDGMENTS

The authors are grateful to Janusz Przeslawski, Marty Gregg, Jim Scott and Yachin Yvry for useful discussions. A.S.E., S.D. and B.N. acknowledge financial support from the alumni organization of the University of Groningen, De Aduarderking (Ubbo Emmius Fonds). Parts of this research were carried out at the light source Petra III at DESY, a member of the Helmholtz Association (HGF). G.C. and N.D. acknowledge projects FIS2015-73932-JIN and MAT2016-77100-C2-1-P from the Spanish MINECO and 2017 -SGR-579 project from the Generalitat de Catalunya. All work at ICN2 is also supported by the Severo Ochoa Program (Grant No. SEV-2017-0706). The work at Penn State is supported by the U.S. Department of Energy, Office of Basic Energy Sciences, Division of Materials Sciences and Engineering under Award FG02-07ER46417 (J.A.Z. and L.Q.C.) and partially by a graduate fellowship from the 3M Company (J. A. Z.).

[1] M. H. Jensen and P. Bak, Physica Scripta **T9**, 64 (1985).

[2] W. Selke, PHYSICS REPORTS **170**, 213 (1988).

[3] Z. Hong, A. R. Damodaran, F. Xue, S. L. Hsu, J. Britson, A. K. Yadav, C. T. Nelson, J. J. Wang, J. F. Scott, L. W. Martin, R. Ramesh, and L. Q. Chen, Nano Letters **17**, 2246 (2017).

[4] P. Shafer, P. García-Fernández, P. Aguado-Puente, A. R. Damodaran, A. K. Yadav, C. T. Nelson, S.-L. Hsu, J. C. Wojdeł, J. Íñiguez, L. W. Martin, E. Arenholz, J. Junquera, and R. Ramesh, Proceedings of the National Academy of Sciences of the United States of America **115**, 915 (2018).

[5] E. K. Salje, Annual Review of Materials Research **42**, 265 (2012).

[6] A. L. Roitburd, Physica Status Solidi (a) **37**, 329 (1976).

[7] W. Pompe, X. Gong, Z. Suo, and J. S. Speck, Journal of Applied Physics **74**, 6012 (1993).

[8] N. A. Pertsev and A. G. Zembilgotov, Journal of Applied Physics **78**, 6170 (1995).

[9] G. Catalan, J. Seidel, R. Ramesh, and J. Scott, Reviews of Modern Physics **84**, 119 (2012).

[10] I. A. Lukyanchuk, A. Schilling, J. M. Gregg, G. Catalan, and J. F. Scott, Physical Review B **79**, 144111 (2009).

[11] A. K. Tagantsev, L. E. Cross, and J. Fousek, *Domains in Ferroic Crystals and Thin Films* (Springer Science + Business Media, Inc., 2011).

[12] A. H. G. Vlooswijk, B. Noheda, G. Catalan, A. Janssens, B. Barcones, G. Rijnders, D. H. A. Blank, S. Venkatesan, B. Kooi, and J. T. M. de Hosson, Applied Physics Letters **91**, 112901 (2007).

[13] L. Feigl, P. Yudin, I. Stolichnov, T. Sluka, K. Shapovalov, M. Mtebwa, C. S. Sandu, X.-K. Wei, A. K. Tagantsev, and N. Setter, Nature communications **5**, 4677 (2014).

[14] J. F. Scott, D. M. Evans, R. S. Katiyar, R. G. P. McQuaid, and J. M. Gregg, Journal of Physics: Condensed Matter **29**, 304001 (2017).

[15] D. D. Fong, G. B. Stephenson, S. K. Streiffer, J. A. Eastman, O. Auciello, P. H. Fuoss, and C. Thompson, Science **304**, 1650 (2004).

[16] G. Catalan, A. Lubk, A. H. G. Vlooswijk, E. Snoeck, C. Magen, A. Janssens, G. Rispens, G. Rijnders, D. H. A. Blank, and B. Noheda, Nature materials **10**, 963 (2011).

[17] P. Gao, J. Britson, C. T. Nelson, J. R. Jokisaari, C. Duan, M. Trassin, S.-H. Baek, H. Guo, L. Li, Y. Wang, Y.-H. Chu, A. M. Minor, C.-B. Eom, R. Ramesh, L.-Q. Chen, and X. Pan, Nature communications **5**, 3801 (2014).

[18] P. Gao, J. Britson, J. R. Jokisaari, C. T. Nelson, S.-H. Baek, Y. Wang, C.-B. Eom, L.-Q. Chen, and X. Pan, Nature communications **4**, 2791 (2013).

[19] A. I. Khan, X. Marti, C. Serrao, R. Ramesh, and S. Salahuddin, Nano Letters **15**, 2229 (2015).

[20] J. C. Agar, A. R. Damodaran, M. B. Okatan, J. Kacher, C. Gammer, R. K. Vasudevan, S. Pandya, R. V. K. Mangalam, G. A. Velarde, S. Jesse, N. Balke, A. M. Minor, S. V. Kalinin, and L. W. Martin, Nature Materials **15**, 549 (2016).

[21] L. J. McGilly, T. L. Burnett, A. Schilling, M. G. Cain, and J. M. Gregg, Physical Review B **85**, 054113 (2012).

[22] M. Takashige, S. Hamazaki, Y. Takahashi, F. Shimizu, and T. Yamaguchi, Japanese Journal of Applied Physics **38**, 5686 (1999).

[23] Y. Ivry, C. Durkan, D. Chu, and J. F. Scott, Advanced Functional Materials **24**, 5567 (2014).

[24] Y. Ivry, D. Chu, J. F. Scott, and C. Durkan, Advanced Functional Materials **21**, 1827 (2011).

[25] R. J. Harrison, S. A. T. Redfern, A. Buckley, and E. K. H. Salje, Journal of Applied Physics **95**, 1706 (2004).

[26] R. J. Harrison, S. A. T. Redfern, and E. K. H. Salje, Physical Review B **69**, 144101 (2004).

[27] A. Schilling, A. Kumar, R. G. P. McQuaid, A. M. Glazer, P. A. Thomas, and J. M. Gregg, Physical Review B **94**, 024109 (2016).

[28] A. L. Tolstikhina, R. V. Gainutdinov, N. V. Belugina, A. K. Lashkova, S. alinin, V. V. Atepalikhin, V. V. Polyakov, and V. A. Bykov, Physica B: Condensed Matter **550**, 332 (2018).

[29] G. Sheng, J. X. Zhang, Y. L. Li, S. Choudhury, Q. X. Jia, Z. K. Liu, and L. Q. Chen, Applied Physics Letters **93**, 232904 (2008).

[30] L. Q. Chen, Journal of the American Ceramic Society **91**, 1835 (2008).

[31] Y. Li, S. Y. Hu, Z. K. Liu, and L. Q. Chen, Applied Physics Letters **81**, 427 (2002).

[32] Y. L. Li and L. Q. Chen, Applied Physics Letters **88**, 072905 (2006).

[33] A. S. Everhardt, S. Matzen, N. Domingo, G. Catalan, and B. Noheda, Advanced Electronic Materials **2**, 1500214 (2016).

[34] V. G. Koukhar, N. A. Pertsev, and R. Waser, Physical Review B **64**, 214103 (2001).

[35] J. J. Wang, P. P. Wu, X. Q. Ma, and L. Q. Chen, Journal of Applied Physics **108**, 114105 (2010).

[36] This is an apparent rule because it ignores the finite width of the b-domains not properly resolved in PFM images.

[37] T. Ozaki, K. Fujii, and J. Ohgami, Journal of the Physical Society of Japan **64**, 2282 (1995).

[38] A. Schilling, T. B. Adams, R. M. Bowman, J. M. Gregg, G. Catalan, and J. F. Scott, Physical Review B **74**, 024115 (2006).

[39] E. K. H. Salje, Journal of Physics: Condensed Matter **5**, 4775 (1993).

[40] I. Tsatskis, E. K. H. Salje, and V. Heine, Journal of Physics: Condensed Matter **6**, 11027 (1994).

[41] J. M. Ball and E. C. M. Crooks, Calculus of Variations and Partial Differential Equations **40**, 501 (2011).

[42] S. Conti, S. Müller, A. Poliakovsky, and E. K. H. Salje, Journal of Physics: Condensed Matter **23**, 142203 (2011).

[43] B. Houchmandzadeh, J. Lajzerowicz, and E. Salje, Journal of Physics: Condensed Matter **3**, 5163 (1991).

[44] B. Houchmandzadeh, J. Lajzerowicz, and E. Salje, Journal of Physics: Condensed Matter **4**, 9779 (1992).

[45] B. Houchmanzadeh, J. Lajzerowicz, and E. Salje, Phase Transitions **38**, 77 (1992).

[46] H. Pöttker and E. K. H. Salje, Journal of Physics: Condensed Matter **26**, 342201 (2014).

[47] E. K. H. Salje, *Phase transitions in ferroelastic and coelastic crystals : an introduction for mineralogists, material scientists, and physicists* (Cambridge University Press, 1993).

[48] A. M. Bratkovsky and A. P. Levanyuk, Physical Review Letters **86**, 3642 (2001).

[49] L. Zuberman, JOURNAL OF MATHEMATICAL ANALYSIS AND APPLICATIONS **474**, 143 (2019).

[50] L. Sun, C. Fang, Y. Song, and Y. Guo, Journal of Physics: Condensed Matter **22**, 445303 (2010).

[51] T. Ozaki and J. Ohgami, Journal of Physics: Condensed Matter **7**, 1711 (1995).

[52] W. van Saarloos and P. Hohenberg, Physica D: Nonlinear

Phenomena **56**, 303 (1992).
[53] G. T. Dee and W. van Saarloos, Physical Review Letters **60**, 2641 (1988).
[54] C. Mathieu, C. Lubin, G. Le Doueff, M. Cattelan, P. Gemeiner, B. Dkhil, E. K. Salje, and N. Barrett, Scientific Reports **8**, 13660 (2018).
[55] N. Barrett, J. Dionot, D. Martinotti, E. K. Salje, and C. Mathieu, Applied Physics Letters **113**, 022901 (2018).
[56] G. F. Nataf, M. Guennou, J. Kreisel, P. Hicher, R. Haumont, O. Aktas, E. K. Salje, L. Tortech, C. Mathieu, D. Martinotti, and N. Barrett, Physical Review Materials **1**, 074410 (2017).
[57] O. Nesterov, S. Matzen, C. Magen, A. H. G. Vlooswijk, G. Catalan, and B. Noheda, Applied Physics Letters **103**, 142901 (2013).
[58] C. S. Ganpule, V. Nagarajan, H. Li, A. S. Ogale, D. E. Steinhauer, S. Aggarwal, E. Williams, R. Ramesh, and P. De Wolf, Applied Physics Letters **77**, 292 (2000).
[59] S. Y. Hu, Y. L. Li, and L. Q. Chen, Journal of Applied Physics **94**, 2542 (2003).
[60] V. Nagarajan, C. S. Ganpule, H. Li, L. Salamanca-Riba, a. L. Roytburd, E. D. Williams, and R. Ramesh, Applied Physics Letters **79**, 2805 (2001).
[61] A. Roelofs, N. A. Pertsev, R. Waser, F. Schlaphof, L. M. Eng, C. Ganpule, V. Nagarajan, and R. Ramesh, Applied Physics Letters **80**, 1424 (2002).
[62] P. D. Scholten and D. R. King, Physical Review B **53**, 3359 (1996).

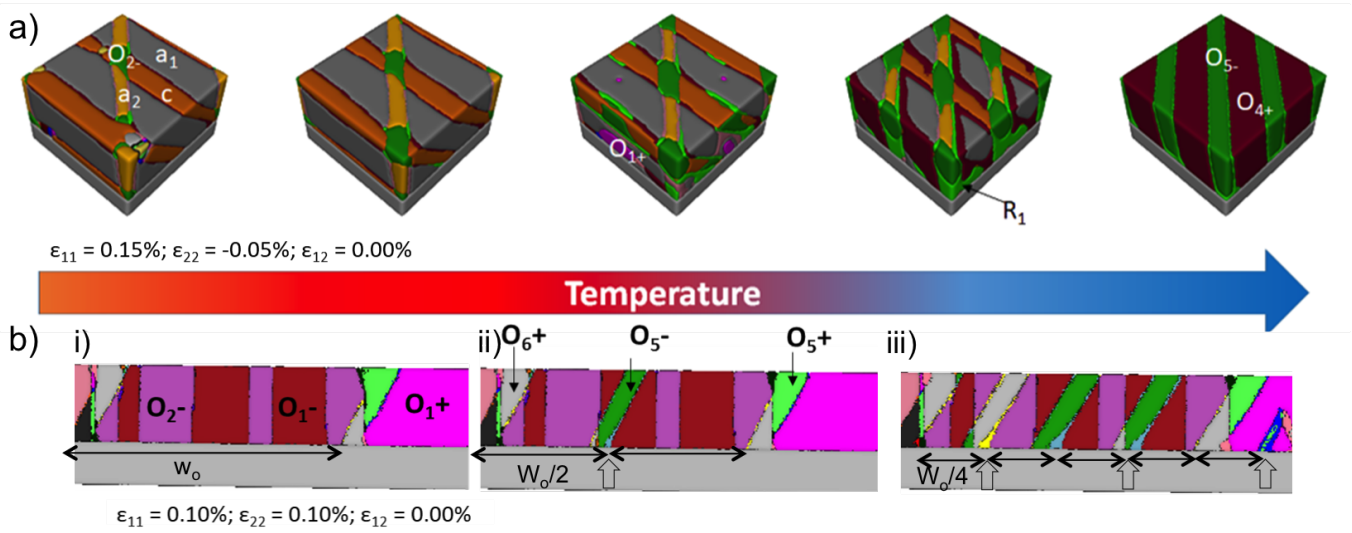

FIG. 5. Three-dimensional (a) and two-dimensional (b) domain structures generated by the phase field method, indicating the misfit strain conditions that led to their formation. In (a), as the temperature decreases from 100°C to 25°C, a change in domain wall orientation from {101} to {110} takes place signalling the phase transition. It is also apparent that the new domains form at the half-way point between the original domain walls. In (b), subsequent nucleation of a new domain halfway between existing domain walls (shown by the open vertical arrows) is also shown to take place as the temperature decreases from 80°C(i) to 60°C (ii) and to 25°C (iii). Domain notation: $a_1 = (P_0, 0, 0)$, $a_2 = (0, P_0, 0)$, $c = (0, 0, P_0)$, $O_{1+} = (P_0, P_0, 0)$, $O_{1-} = (-P_0, -P_0, 0)$, $O_{2+} = (P_0, -P_0, 0)$, $O_{2-} = (-P_0, P_0, 0)$, $O_{4+} = (P_0, 0, -P_0)$, $O_{5+} = (0, P_0, P_0)$, $O_{5-} = (0, -P_0, -P_0)$, $O_{6+} = (0, P_0, -P_0)$, $O_{6-} = (0, -P_0, P_0)$ and $R_1 = (P_0, -P_0, -P_0)$.